Differential study of proton-helium collisions at intermediate energies: Elastic scattering, excitation, and electron capture

K. H. Spicer [ORCID],[*] C. T. Plowman [ORCID], I. B. Abdurakhmanov [ORCID], A. S. Kadyrov [ORCID],[†] and I. Bray [ORCID]

Curtin Institute for Computation and Department of Physics and Astronomy, Curtin University, GPO Box U1987, Perth, WA 6845, Australia

Sh. U. Alladustov [ORCID]

Uzbek-Israel Joint Faculty, National University of Uzbekistan, Tashkent 100174, Uzbekistan

In a series of papers we present a comprehensive investigation of the four-body proton-helium differential scattering problem using the two-center wave-packet convergent close-coupling approach in the intermediate energy region where coupling between various channels is important. The approach uses correlated two-electron wave functions for the helium target. For comparison, a recently developed method that reduces the target to an effective single-electron system is also used. In this paper we present calculations of angular differential cross sections for elastic-scattering, target excitation, and electron-capture processes. The results of the two-electron and effective single-electron methods exhibit a good level of agreement. They also agree well with available experimental data. It is concluded that both versions of the wave-packet convergent close-coupling approach are capable of providing a realistic differential picture of all interdependent and interconnected binary processes taking place in proton-helium collisions at intermediate energies.

I. INTRODUCTION

The study of ion-atom collisions has been, and still is, one of the most intensive areas of research within atomic physics. A complete understanding of processes of excitation, ionization, and charge exchange occurring in collisions is essential for applications in areas such as astrophysics [1] and plasma physics [2]. Such collisional phenomena are also relevant to hadron therapy [3]. Many approaches to modeling such collisions have been developed [4]. For a recent review of energetic ion-atom and ion-molecule collisions, see Ref. [5].

The simplest four-body ion-atom scattering problem is represented by collisions of protons with helium atoms. The proton-helium system has been extensively investigated both experimentally [6–23] and theoretically [24–41] to obtain total and differential cross sections for excitation, electron capture, and ionization. While various theoretical approaches result in the integrated cross sections, e.g., for electron capture, in good agreement with experiment (see [40,41] and references therein), they may lead to quantitatively and qualitatively different predictions of the corresponding differential cross sections. Thus the differential cross sections represent a more stringent test of the theoretical models. Calculations of various differential cross sections provide a complete differential picture of all the interrelated processes occurring in a collision simultaneously. We consider the intermediate energy region where the projectile speed is either comparable to, or somewhat larger than, the electron's orbital speed.

Accordingly, at these energies coupling between various channels cannot be ignored.

A number of methods have been applied to the differential scattering problem. Optical potential methods were employed by Potvliege *et al.* [33] to investigate elastic scattering and by Henne *et al.* [29] to investigate elastic scattering and excitation into $2s$ and $2p$ states at an incident projectile energy of 100 keV. Both methods consistently overestimated the experimental data of Peacher *et al.* [14] for elastic scattering, while reasonable agreement between the results of Henne *et al.* [29] and the experiment of Kvale *et al.* [9] was found for excitation.

Classical-trajectory Monte Carlo (CTMC) calculations of Schultz *et al.* [35] and Lundy *et al.* [30] produced results in good agreement with the experiment of Martin *et al.* [10] for differential electron-capture cross sections into all projectile states at 100 keV. However, the calculation of Lundy *et al.* [30] deviated from the experiment of Seely *et al.* [23] for electron transfer into the $2p$ state as scattering angle increased.

The classical static-potential method employed by Kobayashi and Ishihara [27] was applied to elastic scattering at 25, 50, and 100 keV. Kobayashi and Ishihara [27] found a large discrepancy between the experimental data [14] and their results at 100 keV. These authors also used the Glauber approximation to calculate the differential elastic-scattering cross section. This method gave better agreement with the experimental data in shape, however, the discrepancy in the magnitude remained.

Methods based on the first Born approximation [25,27,31], better suited to higher-energy collisions, achieved certain success in the narrow forward-scattering cone but displayed unphysical dips and disagreement at larger angles. In these works, the results for electron capture into all states were

---

[*]kate.bain@student.curtin.edu.au
[†]a.kadyrov@curtin.edu.au

obtained from the calculations into only the 1*s* state by using the Oppenheimer scaling rule.

A number of other perturbative methods, namely the continuum distorted wave-eikonal initial state (CDW-EIS) method of Abufager *et al.* [24], the four-body final channel distorted-wave method of Halder *et al.* [26], the boundary-corrected four-body continuum-intermediate-state (BCIS) method of Mančev *et al.* [32], the symmetric eikonal two-electron distorted-wave (SE2) method of Rodríguez *et al.* [34], and the distorted-wave Hartree-Fock (DWHF) method of Wong *et al.* [37], have employed the distorted-wave formalism in their calculations for elastic scattering [37], electron capture into the 1*s* state [24,26,32], and excitation into the 2*p* state [34]. All these methods resulted in good agreement with experiments for the particular processes they were applied to, except for the partial-wave method of Wong *et al.* [37] which gave reasonable agreement only after scaling by a factor of 0.1. No justification for such scaling was given.

The perturbative methods mentioned above are applicable at sufficiently high energies. In the intermediate energy range, various reaction channels are interdependent. Therefore, coupling between these channels is important. These effects can be accounted for in the close-coupling formalism. In a two-center atomic-orbital close-coupling (AOCC) approach of Slim *et al.* [36], it was found that the effect of electron exchange has increasing importance with decreasing projectile impact energy. The approach is found to be in good agreement with experimental data for electron capture into all projectile states [10] and excitation into 2*s* and 2*p* states of the target [9], but it showed poor agreement for elastic scattering [14] at a projectile energy of 100 keV. Another coupled-channel approach is the two-center basis generator method (BGM) using an independent-electron model (IEM) and one-active-electron (OAE) model of the helium target by Zapukhlyak *et al.* [39]. The BGM is a nonperturbative coupled-channel method for solving the time-dependent Schrödinger equation where the included basis states gradually adapt to the dynamics of the individual collision system. For comparison they also used the one-active-electron model for helium with a screening potential. Both implementations of the method were used to calculate electron capture into all states of hydrogen over projectile energies ranging from 25 to 200 keV and the results of the calculations were compared with the experimental data. Good agreement was found between the basis generator method results and measurements of Schulz *et al.* [22] at all energies. Good agreement was found also with the experimental data by Schöffler *et al.* [19] and Martin *et al.* [10]; however, agreement was poor with the experiment of Mergel *et al.* [11]. There was a slight difference between the two-electron and one-active-electron basis generator method results, but as projectile energy increases, the results appear to merge.

The close-coupling approaches have certain challenges. In the high-energy regime, the interaction matrix elements become highly oscillatory making numerical evaluations extremely difficult. This may prevent the close-coupling approaches from reaching convergence in terms of the number of the included basis states. There are also challenges with modeling the continuum, restricting the applicability of the close-coupling method, particularly in the energy range considered herein where the probability of capture into the continuum of the projectile cannot be ignored. The convergent close-coupling approach has been developed to circumvent these difficulties using the fully quantum-mechanical [42,43], standard semiclassical [44], and wave-packet [45,46] implementations for the fundamental proton-hydrogen collision system. The wave-packet convergent close-coupling (WP-CCC) method has most recently been applied to the calculation of various singly differential cross sections for the proton-hydrogen system [47] leading to excellent agreement with experiment. The method has also been extended to the proton-helium system in Refs. [48] and [41]. Calculations of the integrated cross sections using this approach agreed very well with experiment in a wide energy range including low, intermediate, and high energies [41].

A brief overview of the theoretical approaches to the differential proton-helium scattering problem given above indicates that different approaches have been applied to isolated reaction channels. Some of them gave very good results for electron capture; however, they cannot provide information on other concurrent channels. There has been no attempt to calculate all the interconnected processes on equal footing at the same time and in a systematic fashion. Our aim here is to fill this gap. We present comprehensive investigation of the four-body proton-helium differential scattering problem using the two-center wave-packet convergent close-coupling approach. The approach uses correlated two-electron wave functions for the helium target. In this paper we focus on the angular differential cross sections for elastic-scattering, target excitation, and electron-capture processes in the intermediate energy (75–300 keV) region where coupling between various channels is important. The aim is to test if the WP-CCC approach is capable of providing a complete differential picture of all the simultaneous interrelated processes occurring during the collision. For comparison, we also use a recently developed approach [49] that allows one to reduce the two-electron helium atom to an effectively single-electron system convenient for scattering calculations. Here we report results for angular differential cross sections for elastic scattering, excitation into the $n = 2$ states (where n is the principal quantum number of the atom in the final state), and state-selective electron capture obtained using both methods. Unless specified otherwise, atomic units (a.u.) are used throughout this manuscript.

II. TWO-CENTER WAVE-PACKET CONVERGENT CLOSE-COUPLING METHOD

A. Correlated two-electron treatment of the helium target

Various aspects of the two-center wave-packet convergent close-coupling method for ion-atom collisions are described in detail in our earlier works [41,46,48,50,51]. The approach has been extended to multicharged projectiles in [52,53] and to two-electron targets in [41]. A brief description of the method is given here with emphasis on the parts relevant to the present calculations.

We apply the frozen-core approximation for the helium target and the semiclassical approximation for the scattering, which are valid at the energies we perform our present calculations. The exact nonrelativistic time-independent Schrödinger

equation for the total scattering wave function Ψ is

$$(H - E)\Psi = 0, \tag{1}$$

where H is the full four-body Hamiltonian and E is the total energy of the collision system. The total Hamiltonian can be split into kinetic-energy and Coulomb interaction potential operators to be

$$H = K_\sigma + H_{T_1} + H_{T_2} + V_P + V_{12}, \tag{2}$$

$$= K_{\rho_1} + H_{P_1} + H_{T_2} + V_1 + V_{12}, \tag{3}$$

$$= K_{\rho_2} + H_{P_2} + H_{T_1} + V_2 + V_{12}, \tag{4}$$

where

$$K_\sigma = -\frac{\nabla_\sigma^2}{2\mu_T}, \quad K_{\rho_i} = -\frac{\nabla_{\rho_i}^2}{2\mu_P}, \quad i = 1, 2, \tag{5}$$

μ_T is the reduced mass of the p-He system, and μ_P is the reduced mass of the H-He$^+$ system. Note that the mass polarization term in the total Hamiltonian is neglected since $\mu_T \gg 1$ and $\mu_P \gg 1$. The interaction potentials are written as

$$V_P = \frac{2}{R} - \frac{1}{x_1} - \frac{1}{x_2}, \tag{6}$$

$$V_1 = \frac{2}{R} - \frac{2}{r_2} - \frac{1}{x_1}, \tag{7}$$

$$V_2 = \frac{2}{R} - \frac{2}{r_1} - \frac{1}{x_2}, \tag{8}$$

$$V_{12} = \frac{1}{|\mathbf{r}_1 - \mathbf{r}_2|}. \tag{9}$$

Here, the position vectors of the incident proton and the two electrons relative to the helium nucleus are $\mathbf{R}$, $\mathbf{r}_1$, and $\mathbf{r}_2$, respectively, and the position vectors of the electrons relative to the incident proton are $\mathbf{x}_1$ and $\mathbf{x}_2$. The position vector of the proton relative to the center of mass of the helium atom is $\boldsymbol{\sigma}$ and the position vector of the proton and first (second) electron system relative to the helium ion is $\boldsymbol{\rho}_1$ ($\boldsymbol{\rho}_2$).

The Hamiltonians of the hydrogen atom formed after electron transfer and the residual helium ion can be written as

$$H_{P_i} = -\frac{\nabla_{x_i}^2}{2} - \frac{1}{x_i}, \quad i = 1, 2, \tag{10}$$

$$H_{T_i} = -\frac{\nabla_{r_i}^2}{2} - \frac{2}{r_i}, \quad i = 1, 2. \tag{11}$$

Using these equations the helium atom Hamiltonian becomes

$$H_T = H_{T_1} + H_{T_2} + V_{12}. \tag{12}$$

We assume the target nucleus is located at the origin and the projectile is moving along the trajectory $\mathbf{R} \equiv \mathbf{R}(t) = \mathbf{b} + \mathbf{v}t$, where $\mathbf{b}$ is the impact parameter and $\mathbf{v}$ is the initial velocity of the projectile relative to the target. The impact parameter vector is perpendicular to the velocity vector, such that $\mathbf{b} \cdot \mathbf{v} = 0$. Then assuming the total electronic spin of helium is conserved throughout the collision, the total scattering wave function is expanded in terms of N target-centered and M projectile-centered pseudostates as

$$\Psi = \sum_{\alpha=1}^{N} a_\alpha(t, \mathbf{b}) \psi_\alpha^{\mathrm{He}}(\mathbf{r}_1, \mathbf{r}_2) e^{i\mathbf{k}_\alpha \boldsymbol{\sigma}}$$

$$+ \frac{1}{\sqrt{2}} \sum_{\beta=1}^{M} b_\beta(t, \mathbf{b}) \big[\psi_\beta^{\mathrm{H}}(\mathbf{x}_1) \psi_{1s}^{\mathrm{He}^+}(\mathbf{r}_2) e^{i\mathbf{k}_{1\beta} \boldsymbol{\rho}_1}$$

$$+ \psi_\beta^{\mathrm{H}}(\mathbf{x}_2) \psi_{1s}^{\mathrm{He}^+}(\mathbf{r}_1) e^{i\mathbf{k}_{2\beta} \boldsymbol{\rho}_2} \big], \tag{13}$$

where the indices α and β denote, respectively, a quantum state in the p-He channel and the H-He$^+$ rearrangement channel, formed after electron capture by the projectile. Accordingly, $\mathbf{k}_\alpha$ is the momentum of the projectile relative to the helium atom in the α channel. Similarly, $\mathbf{k}_{1\beta}$ ($\mathbf{k}_{2\beta}$) is the momentum of the hydrogen atom relative to the residual helium ion in the 1β (2β) channel. Channels 1β and 2β are the same but have the electron of the hydrogen atom and the electron of the residual helium ion exchanged. Thus our method accounts for the exchange effects between the captured electron and the electron of the residual He$^+$ ion. In the above equation, $\psi_\alpha^{\mathrm{He}}$ and ψ_β^{H} are the wave functions of the helium and hydrogen atoms, respectively, and $\psi_{1s}^{\mathrm{He}^+}$ is the ground-state wave function for the helium ion. The expansion coefficients $a_\alpha(t, \mathbf{b})$ and $b_\beta(t, \mathbf{b})$ represent the transition amplitudes into the corresponding final channel as $t \to +\infty$.

We substitute the expansion in Eq. (13) into Eq. (1) and successively multiply all terms of the resulting equation by $\psi_{\alpha'}^{\mathrm{He}*}(\mathbf{r}_1, \mathbf{r}_2) e^{-i\mathbf{k}_{\alpha'} \boldsymbol{\sigma}}$ for $\alpha' = 1, \dots, N$ and $\psi_{\beta'}^{\mathrm{H}*}(\mathbf{x}_1) \psi_{1s}^{\mathrm{He}^+}(\mathbf{r}_2) e^{-i\mathbf{k}_{1\beta'} \boldsymbol{\rho}_1} + \psi_{\beta'}^{\mathrm{H}*}(\mathbf{x}_2) \psi_{1s}^{\mathrm{He}^+}(\mathbf{r}_1) e^{-i\mathbf{k}_{2\beta'} \boldsymbol{\rho}_2}$ for $\beta' = 1, \dots, M$. Then using the semiclassical approximation, where the action of the ∇^2 operator on the expansion coefficients a_α and b_β is neglected as they vary slowly with $\boldsymbol{\sigma}$ and $\boldsymbol{\rho}_i$, respectively, and integrating over all variables except for $\boldsymbol{\sigma}$, $\boldsymbol{\rho}_1$, and $\boldsymbol{\rho}_2$, we obtain a set of coupled first-order differential equations for the time-dependent coefficients:

$$i\dot{a}_{\alpha'} + i \sum_{\beta=1}^{M} \dot{b}_\beta K_{\alpha'\beta}^T = \sum_{\alpha=1}^{N} a_\alpha D_{\alpha'\alpha}^T + \sum_{\beta=1}^{M} b_\beta Q_{\alpha'\beta}^T,$$

$$i \sum_{\alpha=1}^{N} \dot{a}_\alpha K_{\beta'\alpha}^P + i \sum_{\beta=1}^{M} \dot{b}_\beta L_{\beta'\beta}^P = \sum_{\alpha=1}^{N} a_\alpha Q_{\beta'\alpha}^P + \sum_{\beta=1}^{M} b_\beta D_{\beta'\beta}^P,$$

$$\alpha' = 1, 2, \dots, N, \quad \beta' = 1, 2, \dots, M. \tag{14}$$

The direct scattering (collectively referring to elastic scattering and target excitation) matrix elements are given by

$$L_{\beta'\beta}^P = \frac{1}{2} \sum_{i,j=1,2} \langle \mathbf{k}_{i\beta'}, \psi_{\beta'}^{\mathrm{H}}, \psi_{1s}^{\mathrm{He}^+} | \psi_\beta^{\mathrm{H}}, \psi_{1s}^{\mathrm{He}^+}, \mathbf{k}_{j\beta} \rangle, \tag{15}$$

$$D_{\alpha'\alpha}^T = \langle \mathbf{k}_{\alpha'}, \psi_{\alpha'}^{\mathrm{He}} | H_T - E_\alpha^{\mathrm{He}} + V_P | \psi_\alpha^{\mathrm{He}}, \mathbf{k}_\alpha \rangle, \tag{16}$$

$$D_{\beta'\beta}^P = \frac{1}{2} \sum_{i,j=1,2} \langle \mathbf{k}_{i\beta'}, \psi_{\beta'}^{\mathrm{H}}, \psi_{1s}^{\mathrm{He}^+} | H_{Pi} - \varepsilon_\beta^{\mathrm{H}} | \psi_\beta^{\mathrm{H}}, \psi_{1s}^{\mathrm{He}^+}, \mathbf{k}_{j\beta} \rangle$$

$$+ \frac{1}{2} \sum_{i,j=1,2} \langle \mathbf{k}_{i\beta'}, \psi_{\beta'}^{\mathrm{H}}, \psi_{1s}^{\mathrm{He}^+} | V_i | \psi_\beta^{\mathrm{H}}, \psi_{1s}^{\mathrm{He}^+}, \mathbf{k}_{j\beta} \rangle. \tag{17}$$

Rearrangement (i.e., electron transfer) matrix elements are given as

$$K_{\beta'\alpha}^{P} = \frac{1}{\sqrt{2}} \sum_{i=1,2} \langle \boldsymbol{k}_{i\beta'}, \psi_{\beta'}^{H}, \psi_{1s}^{He^{+}} | \psi_{\alpha}^{He}, \boldsymbol{k}_{\alpha} \rangle, \qquad (18)$$

$$K_{\alpha'\beta}^{T} = \frac{1}{\sqrt{2}} \sum_{i=1,2} \langle \boldsymbol{k}_{\alpha'}, \psi_{\alpha'}^{He} | \psi_{\beta}^{H}, \psi_{1s}^{He^{+}}, \boldsymbol{k}_{i\beta} \rangle, \qquad (19)$$

$$Q_{\beta'\alpha}^{P} = \frac{1}{\sqrt{2}} \sum_{i=1,2} \langle \boldsymbol{k}_{i\beta'}, \psi_{\beta'}^{H}, \psi_{1s}^{He^{+}} | H_{T} - E_{\alpha}^{He} + V_{P} | \psi_{\alpha}^{He}, \boldsymbol{k}_{\alpha} \rangle, \qquad (20)$$

$$Q_{\alpha'\beta}^{T} = \frac{1}{\sqrt{2}} \sum_{i=1,2} \langle \boldsymbol{k}_{\alpha'}, \psi_{\alpha'}^{He} | H_{Pi} - \varepsilon_{\beta}^{H} + V_{i} | \psi_{\beta}^{H}, \psi_{1s}^{He^{+}}, \boldsymbol{k}_{i\beta} \rangle. \qquad (21)$$

Here, E_{α}^{He} is the total energy of He in state α and ε_{β}^{H} is the energy of hydrogen in state β. Further details can be found in Ref. [41].

The system of equations (14) is solved subject to the initial boundary condition

$$a_{\alpha}(-\infty, \boldsymbol{b}) = \delta_{\alpha,1s}, \quad \alpha = 1, \dots, N,$$
$$b_{\beta}(-\infty, \boldsymbol{b}) = 0, \quad \beta = 1, \dots, M, \qquad (22)$$

which assumes that the active target electron is initially in the 1*s* orbital.

Once the time-dependent expansion coefficients are found, the differential cross sections for direct scattering (DS) and electron capture (EC) from the initial state *i* to the final state *f* are calculated as

$$\frac{d\sigma_{fi}^{DS(EC)}}{d\Omega} = \frac{\mu_{T}\mu_{f}}{(2\pi)^{2}} \frac{q_{f}}{q_{i}} |T_{fi}^{DS(EC)}(\boldsymbol{q}_{f}, \boldsymbol{q}_{i})|^{2}, \qquad (23)$$

where $\Omega = (\theta, \phi)$ is the solid angle of $\boldsymbol{q}_{f}$ (relative to $\boldsymbol{q}_{i}$). We choose the target to be in its ground state in the initial channel. Therefore, we set $\boldsymbol{q}_{i} = \boldsymbol{k}_{1}$; however, $\boldsymbol{q}_{f} = \boldsymbol{k}_{\alpha'}$ or $\boldsymbol{q}_{f} = \boldsymbol{k}_{1\beta'} \equiv \boldsymbol{k}_{2\beta'}$ depending on the type of scattering. Accordingly, reduced mass $\mu_{f} = \mu_{T}$ for the *p*-He channel and $\mu_{f} = \mu_{P}$ for the H-He^{+} channel. The direct scattering (elastic scattering or excitation) amplitudes T_{fi}^{DS} and electron-capture amplitudes T_{fi}^{EC} are calculated from the impact-parameter space transition probability amplitudes as follows:

$$T_{fi}^{DS}(\boldsymbol{q}_{f}, \boldsymbol{q}_{i}) = 2\pi i v \, e^{im\phi_{f}} \int_{0}^{\infty} db \, b [\tilde{a}_{f}(+\infty, b) - \delta_{fi}] J_{m}(q_{\perp}b) \qquad (24)$$

and

$$T_{fi}^{EC}(\boldsymbol{q}_{f}, \boldsymbol{q}_{i}) = 2\pi i v \, e^{im\phi_{f}} \int_{0}^{\infty} db \, b \, \tilde{b}_{f}(+\infty, b) J_{m}(q_{\perp}b), \qquad (25)$$

where $q_{\perp}$ is the magnitude of the perpendicular component of the momentum transfer $\boldsymbol{q} = \boldsymbol{q}_{i} - \boldsymbol{q}_{f}$, *m* is the magnetic quantum number of the bound state in the final channel, ϕ_{f} is the azimuthal angle of $\boldsymbol{q}_{f}$, and J_{m} is the Bessel function of the *m*th order. For details of the above procedures we refer to Sec. 3.8 of Ref. [4]. The probability amplitudes are related to the expansion coefficient as

$$\tilde{a}_{f}(t, b) = e^{im\phi_{b}} a_{f}(t, \boldsymbol{b}) \qquad (26)$$

and

$$\tilde{b}_{f}(t, b) = e^{im\phi_{b}} b_{f}(t, \boldsymbol{b}), \qquad (27)$$

where ϕ_{b} is the azimuthal angle of $\boldsymbol{b}$.

B. Effective single-electron treatment of the helium target

Proton scattering on a two-electron system is a complex problem to solve due to the electron-electron correlations and exchange effects between the captured electron and the electron of the residual helium ion which belong to different centers. A comprehensive two-electron treatment of the problem, similar to the one described in the previous section, is very involved theoretically and time consuming computationally. On the other hand, there are no such complications in the case of bare-ion collisions with a hydrogenlike system. Therefore, for comparison we also perform calculations using a recently developed method [49] that allows one to reduce the two-electron target to an effective single-electron system. Then we can take advantage of our existing numerical methods that have been implemented for bare-ion collisions with one-electron targets and reduce the amount of required computational resources when calculating cross sections.

Below we briefly summarize the effective single-electron (E1E) technique. First we utilize a computational atomic-structure package based on the multiconfiguration Hartree-Fock approximation to produce an accurate multielectron wave function for the ground state of a particular atom. Using the obtained ground-state wave function we calculate the probability density for the whole atom. Next we average this density function over the spatial coordinates and spin variables of all the target electrons except for the distance of any one electron from the nucleus. The resulting single-electron density function represents the probability of finding one electron of the target at a certain distance from the target nucleus. For the ground state this function is generally nodeless and, therefore, its positive (or, equivalently, negative) square root defines the corresponding single-electron wave function. Inserting the latter into the multielectron Schrödinger equation for the target reduces it to effectively a single-electron equation and allows us to calculate an effective potential representing the collective field produced by the target nucleus and all the other target electrons. With the known ground-state radial wave function, the effective potential can be found by inversely solving the reduced Schrödinger equation. Then the reduced Schrödinger equation is used to find radial wave functions for the excited bound states and the continuum state of the active electron. In the next step, following the wave-packet continuum discretization approach, the resulting continuum is used to construct wave-packet pseudostates. These pseudostates are square integrable and well suited for scattering calculations. Eventually, radial functions of the ground state, several excited states, and wave-packet pseudostates form a basis which describes the multielectron atomic target. One should note that the effective potential of the target core found this way takes into account the possibility of excitations of not only the outermost electron but all electrons of the multielectron atom. In this work we apply this procedure to the two-electron helium atom. The wave-packet continuum discretization for hydrogenlike ions is described in Ref. [45].
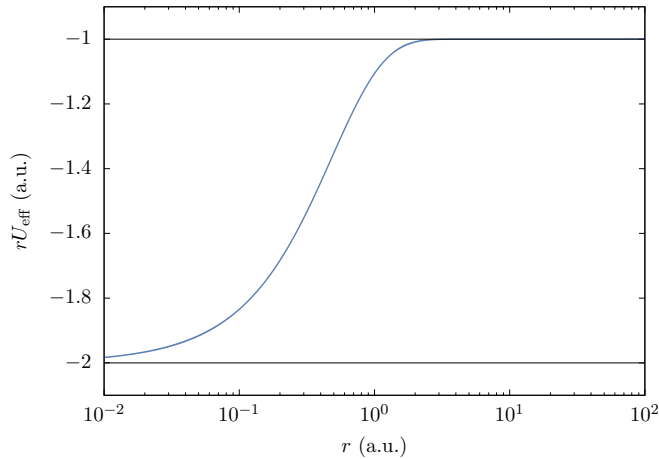
FIG. 1. Effective potential $U_{eff}(r)$ weighted by radius r as a function of r for helium.

Thus, in our case, the effective potential represents the collective field produced by the target nucleus and the second electron of the target. Figure 1 shows the radial dependence of the effective potential $U_{eff}(r)$ multiplied by radius r for the helium atom. Here $U_{eff}(r)$ is the potential which is felt by any one of the electrons in the field produced by the nucleus and the remaining electron of the atom. As we can see the potential is attractive, and tends to the expected functional form of $-2/r$ near the origin and has the asymptotic $-1/r$ tail at large distances.

The radial wave functions and corresponding energies for the excited states and continuum states of the multielectron atom are found by solving the reduced single-electron Schrödinger equation for each angular momentum l using the Numerov method. The bound states are found by utilizing a standard shooting method. The resulting states form a set of negative-energy pseudostates approximately representing the target space, including the ground state that is accurate by construction. For the continuum states, the radial wave function is matched to the Coulomb function at large r, which is also used to derive the continuum phase shift. The radial functions for the bound states are normalized. The continuum wave function is normalized to the Dirac delta function. Finally, we use the wave-packet continuum-discretization approach to generate pseudostates. The procedure is similar to the one recently applied to describe the structure of atomic hydrogen [45]; however, the continuum solution comes in a numerical form.

III. CALCULATIONS OF ANGULAR DIFFERENTIAL CROSS SECTIONS

Below we present the differential cross sections for binary reactions (elastic scattering, target excitation, and electron capture) at four intermediate incident energies: 75, 100, 150, and 300 keV. Our main results obtained using the correlated two-electron wave-packet convergent close-coupling approach are denoted as WP-CCC. For comparison we also present results obtained using the effective single-electron treatment of the helium target described in Sec. II B. In both

approaches the number of included negative- and positive-energy pseudostates are increased until adequate convergence is achieved in the predicted cross sections for the collision process that we are interested in.

The set of equations (14) for the expansion coefficients, representing the transition amplitudes, was solved using the Runge-Kutta method by incrementing the position of the projectile along the $z = v_0 t$ axis in the scattering plane from $z_{min} = -100$ a.u. to $z_{max} = 100$ a.u. for all impact parameters. The exponential z grid, with denser discretization around $z = 0$, contains 200 points. Checks showed that the difference between the 200-point and 400-point results was insignificant. The numerical quadrature used in Eqs. (24) and (25) for integration over the impact parameter was the Gauss-Legendre quadrature. The impact parameters ranged from 0 up to 30 a.u., which was sufficient to allow for the probability of all the processes being investigated to fall off several orders of magnitude. The maximum impact parameter was increased to 40 a.u. to remove oscillations for excitation into the $2p$ state. Increasing the maximum impact parameter further made no significant contribution to the results. Integration over the impact parameter was performed with 128 quadrature points. The results were checked for accuracy using 16, 32, and 64 points. There was no difference between the 64-point and 128-point results reported in this work.

For discretization of the continuum, the maximum momentum of the ejected electron κ_{max} was increased systematically until no further change in the results was observed. Maximum momentum $\kappa_{max} = 5$ a.u. was verified to be sufficient for all the angular differential cross sections considered in this work to converge at intermediate energies. This corresponds to the maximum energy of the ejected electrons ε_{max} to be about 340 eV, where the singly differential cross sections for ionization at all considered impact energies fall off at least three orders of magnitude.

To achieve convergence in all the cross sections calculated, it was found that a basis containing the bound states up to the principal quantum number 5 and 20 bin states on both centers was more than sufficient. The maximum orbital angular momentum for both negative-energy and positive-energy states was 3. Angular differential cross sections are calculated from the transition amplitudes for the corresponding states using Eq. (25).

A. Differential cross sections for elastic scattering and target excitation

The angular differential cross sections for elastic scattering (denoted as $1s$), target excitation into the $2s$ and $2p$ states, and the $n = 2$ shell obtained with the two-electron WP-CCC approach are presented in Fig. 2 in comparison with experimental data [9,14,20] and other calculations [27,34,36,37]. The results are presented in the center-of-mass frame (where the center of mass of the proton-helium system is at rest). As seen from the figure, the two-electron WP-CCC results agree very well with the experimental data, where available, for all processes except for elastic scattering. For comparison results obtained using the effective single-electron treatment of the helium target are also shown. As one can see, the
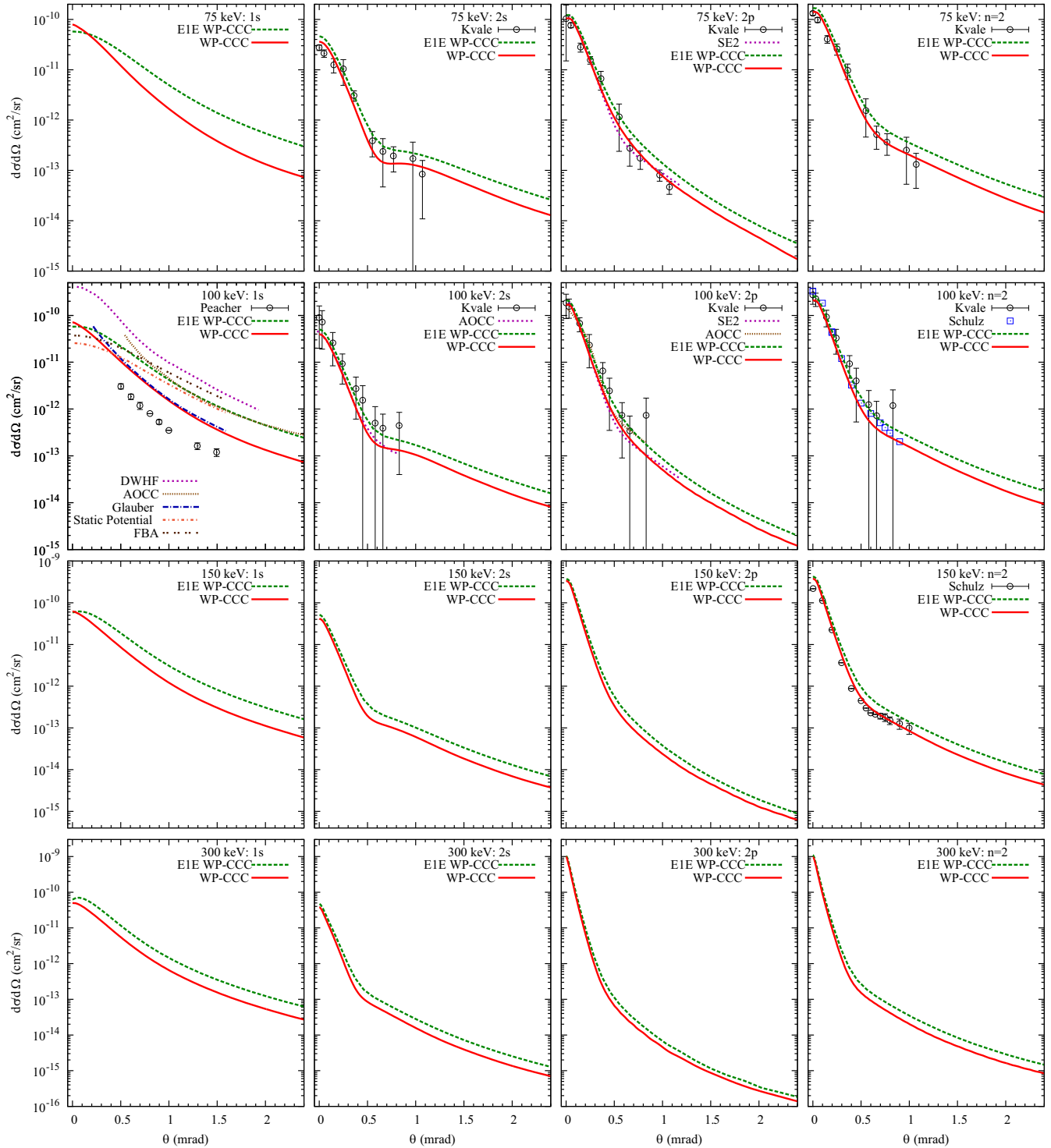
FIG. 2. State-selective angular differential cross sections for elastic (1s) scattering and target excitation in proton-helium collisions as functions of scattering angle in the center-of-mass frame. Projectile energies are 75, 100, 150, and 300 keV. Experimental data by Peacher *et al.* [14], Kvale *et al.* [9], and Schulz *et al.* [20] are shown in the corresponding panels. Theoretical results are the present two-electron WP-CCC approach, the distorted-wave Hartree-Fock (DWHF) approach of Wong *et al.* [37], the atomic-orbital close-coupling (AOCC) method of Slim *et al.* [36], the symmetric eikonal distorted-wave (SE2) approach by Rodríguez *et al.* [34], and the Glauber approximation and the classical static-potential methods by Kobayashi and Ishihara [27]. The present E1E WP-CCC results are also shown.

E1E WP-CCC results also show reasonable agreement, again except for elastic scattering.

For elastic scattering at 100 keV, the two-electron WP-CCC results come closer to the experimental data by Peacher

et al. [14] than the other calculations [36,37] including the present E1E WP-CCC ones. Our two-electron WP-CCC results agree with the calculations by Kobayashi and Ishihara [27] based on the Glauber approximation within the

angular range from 0.5 to 1.5 mrad. Overall, there is still significant disagreement between experiment and theory (theory in general). Previously, the failure of the theoretical treatments to adequately account for the effects of the various inelastic channels, particularly ionization and charge transfer, was suggested to be a possible source of the discrepancy between the theoretical results and the only experiment available on elastic scattering by Peacher *et al.* [14]. Therefore, we expected that including a sufficient number of negative-energy and positive-energy pseudostates would resolve the discrepancy as such a large basis correctly accounts for the polarizability of the target. However, as we can see from the figure, this is not the case. As Peacher *et al.* [14] mentioned, relative data from their experimental chamber, the interaction length of which was uncertain, were normalized to the absolute differential cross sections using a single normalizing constant. Given the two-electron WP-CCC method is based on the very accurate correlated two-electron target structure and the obtained results are convergent in terms of the included target- and projectile-centered states, one can cautiously suggest that there could be a normalization error in the experiment. Indeed, agreement in shape between the experiment and the two-electron WP-CCC results is excellent. Note that there was no such disagreement in similar calculations for the proton-hydrogen system [47].

Excitation into the 2*s* state sees greater similarity between the E1E and two-electron WP-CCC methods. The two sets of results are very close to each other near the forward direction across all energies. However, the E1E WP-CCC results overestimate the two-electron WP-CCC calculations for larger scattering angles with the difference between the two methods decreasing as projectile energy increases. Nevertheless, both two-electron and E1E WP-CCC calculations agree very well with the experimental results by Kvale *et al.* [9] available at 75 and 100 keV and for scattering angles up to 1.07 and 0.83 mrad, respectively. The AOCC calculation by Slim *et al.* [36] at 100 keV also agrees well with the experiment, following a very similar pattern as the two-electron WP-CCC method within the angular range where the data are available. The cross section for 2*p* excitation is the combination of the cross sections for excitation into the $2p_{-1}$, $2p_0$, and $2p_1$ states. Here, the situation is very similar to that of 2*s* excitation. Rodríguez *et al.* [34] performed symmetric eikonal distorted-wave calculations at 75 and 100 keV for scattering angles up to 0.5 mrad. Their results agree very well with our two-electron WP-CCC calculations. Again, the E1E WP-CCC 2*p* angular cross section is somewhat higher than the more accurate two-electron one away from the forward direction, but the difference between the E1E and two-electron results is still within the experimental uncertainties. For excitation into all the states of the $n = 2$ shell combined, there is another set of measurements by Schulz *et al.* [20] at 100 and 150 keV. The two-electron WP-CCC results describe the Schulz *et al.* [20] data very well.

B. Differential cross sections for electron capture

The angular differential cross sections for electron capture into 1*s*, 2*s*, and 2*p* states of the projectile as well as those summed over all the included bound states on

the projectile center are shown in Fig. 3. We present the results obtained with the two-electron WP-CCC approach together with experimental data [8,10,11,19,22,23] and other calculations [24,32,35,39]. Similar to elastic scattering and target excitation, results are presented in the center-of-mass frame. For comparison results obtained using the effective single-electron treatment of the helium target are also shown. Generally, the state-selective and total electron-capture cross sections obtained using both two-electron and E1E WP-CCC methods agree well with the experimental results, where available.

Schöffler *et al.* [19] reported the angular-differential cross section for electron capture into the ground state of helium using the cold target recoil ion momentum spectroscopy technique. The E1E and two-electron WP-CCC methods are in excellent agreement with their data over the entire angular and energy ranges, especially for small scattering angles less than 0.5 mrad. At very small scattering angles our results agree with the CTMC calculation of Schultz *et al.* [35] available at 100 keV. Agreement is reasonably good also at larger angles with some deviation between 0.4 and 1.2 mrad. The boundary-corrected first Born approximation (CB1) and the BCIS methods of Mančev *et al.* [32], being perturbative in nature, predict unphysical dips around 0.4 and 0.8 mrad, respectively. They agree with the data in the narrow forward cone which should ensure the resulting integrated cross section is accurate.

For capture into the 2*s* state of hydrogen, the two-electron and E1E WP-CCC methods are very close to each other over the entire angular range. No experimental data is available for this process. The CTMC calculations by Schultz *et al.* [35] are available at 100 keV. The difference between the CTMC results and the WP-CCC ones is somewhat similar to the situation with ground-state capture. For capture into the 2*p* state of hydrogen, the two-electron and E1E WP-CCC methods are in agreement for scattering angles less than ∼0.5 mrad after which they slightly deviate from each other. The experiment was conducted by Seely *et al.* [23] for 100 keV. The two-electron and E1E WP-CCC results do not agree well with the experiment [23], overestimating it for scattering angles near the forward direction and underestimating it at larger angles. The CTMC results by Schultz *et al.* [35] are in somewhat better agreement with the experiment but still do not correctly reproduce the shape of the cross section, underestimating the experiment at small angles and overestimating it at larger angles. As a matter of fact, we note that the two-electron WP-CCC results at 25 keV are in very good agreement with the corresponding measurements by Seely *et al.* [23], but at 50 keV agreement is already not good, just like at 100 keV (not shown).

The two-electron and E1E WP-CCC results for the total cross sections for electron capture into all included projectile states are compared with the experiments of Guo *et al.* [8], Schulz *et al.* [22], Mergel *et al.* [11], and Martin *et al.* [10], along with the CTMC calculations of Schultz *et al.* [35], and the CDW-EIS method of Abufager *et al.* [24], the CB1 and BCIS results of Mančev *et al.* [32], and the BGM IEM results of Zapukhlyak *et al.* [39]. At 100 keV, the CTMC results of Schultz *et al.* [35] are in very good agreement with the experiment at all angles. Our results are in excel-
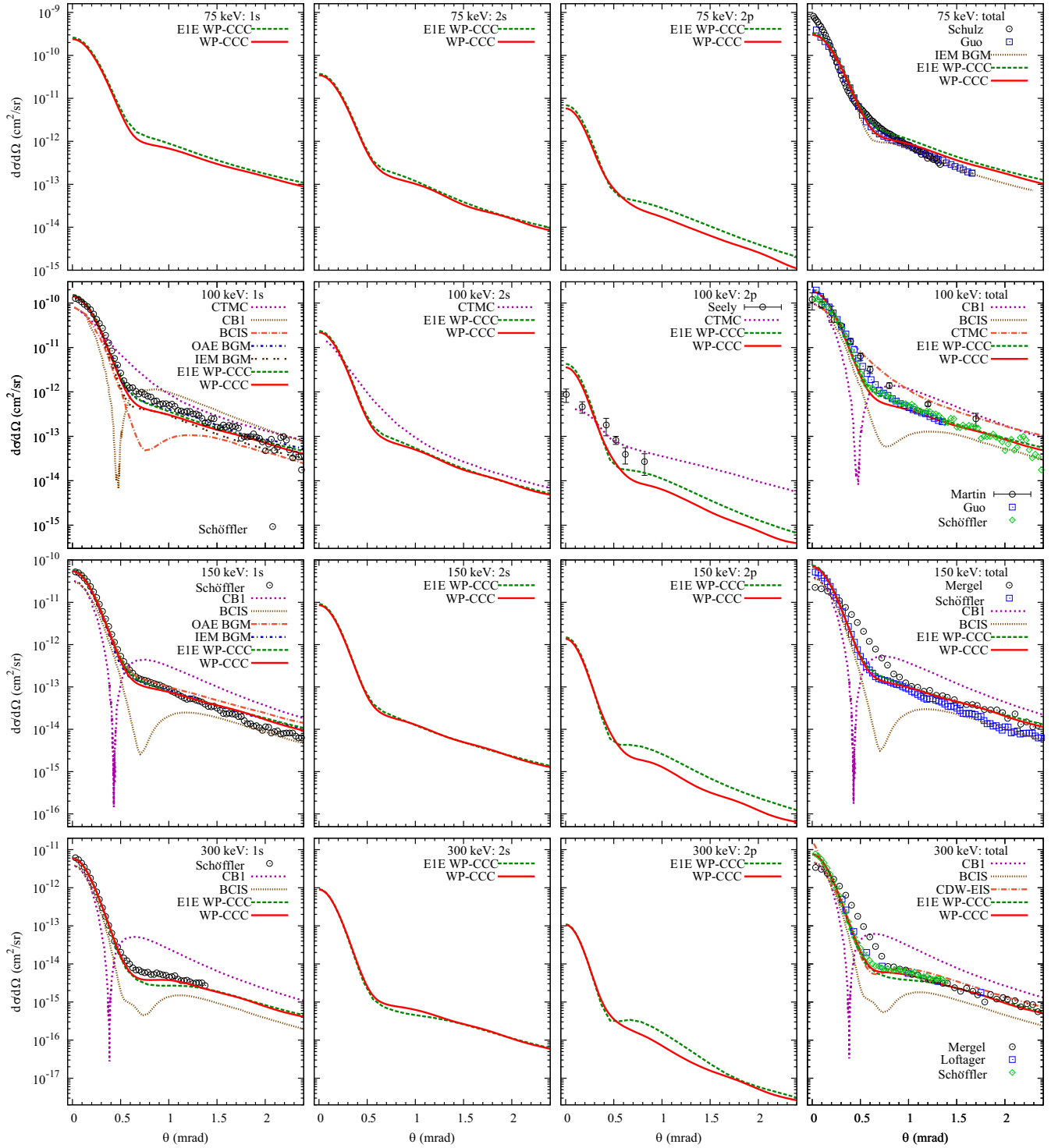
FIG. 3. State-selective and total angular differential cross sections for electron capture in proton-helium collisions as functions of scattering angle in the center-of-mass frame. Projectile energies are 75, 100, 150, and 300 keV. Experimental data by Schöffler *et al.* [19], Mergel *et al.* [11], Seely *et al.* [23], Guo *et al.* [8], Schulz *et al.* [22], Martin *et al.* [10], and Loftager (reported in Ref. [31]) are shown in the respective panels. Theoretical results are the present two-electron WP-CCC approach, the classical trajectory Monte Carlo (CTMC) method by Schultz *et al.* [35], the corrected first Born (CB1) and boundary-corrected intermediate-state (BCIS) methods of Mančev *et al.* [32], the continuum distorted wave-eikonal initial state (CDW-EIS) method of Abufager *et al.* [24], and the two-center basis generator method (BGM) using the independent-electron model (IEM) and one-active-electron model (OAE) for He by Zapukhlyak *et al.* [39]. The present E1E WP-CCC results are also shown.

lent agreement with the most recent measurements by Guo *et al.* [8]. They also agree well with the earlier data by Martin *et al.* [10] and Schulz *et al.* [22]. However, they do not support the Mergel *et al.* [11] data. For comparison we plot the ground-state capture cross sections by Schöffler *et al.* [19] believed to be more accurate. Given the fact the ground-state capture cross section gives about 80% of the total, we see a possible problem with the Mergel *et al.* [11] data. The latter significantly underestimates the ground-state data in a narrow cone around the forward direction (that defines the integrated capture cross section) and predicts a different slope. One can notice that the difference between the two-electron and E1E WP-CCC results is quite small meaning that the effective one-electron treatment of the He target is acceptable for total electron capture at least in the intermediate energy range considered here. A similar conclusion was drawn [39] based on the IEM and OAE implementations of the BGM method. Furthermore, we observe generally good agreement between the WP-CCC and IEM BGM results. We should note that the BGM approach with the OAE model of He is conceptually similar to our E1E WP-CCC approach. At the same time, comparison of the present two-electron WP-CCC cross sections with the results of the BGM approach based on the independent-electron model should give information about the role of electron correlation effects. However, we should also consider differences in the methodology that contribute to observed deviation.

Overall, nonperturbative methods describe the experiment well. Note that our calculations show no evidence of any significant contribution to electron capture from the Thomas double-scattering mechanism in the energy range considered here. However, this mechanism is expected to become important as the incident energy increases and this should show up in the differential cross sections for electron capture [54,55] and ionization. We consider this case elsewhere.

We note that our method includes all interaction potentials. Some authors mentioned above solve the semiclassical Schrödinger equation without the internuclear potential and incorporate the latter in the form of a phase factor. The WP-CCC method is based on the full Schrödinger equation with the full four-body Hamiltonian. Finally, we remark that in all cases the differential cross sections display somewhat similar behavior. They fall off fast at small angles. This changes around 0.5–0.75 mrad beyond which the fall off is slower. Larger scattering angles correspond to smaller impact parameters and vice versa. Accordingly, scattering into large angles is mostly due to the heavy-particle interaction at short distances while the electron interaction with the projectile and the target nucleus is responsible for scattering into small angles where collision takes place at relatively long distances.

IV. CONCLUSION

The two-center wave-packet convergent close-coupling approach based on the correlated two-electron treatment of the target was applied to calculate angular differential cross sections for elastic scattering, target excitation, and electron capture in proton-helium collisions at intermediate projectile energies. Results for the angular differential cross sections of excitation and electron capture agree well with experiment. For elastic scattering, there is significant disagreement between the only available experiment at 100 keV and theory, though agreement in shape between the experiment and the two-electron WP-CCC results is excellent. We cannot explain the discrepancy. New experiments and independent calculations would shed more light on the situation. We also present results using a recently developed effective single-electron description of the target. Results from this alternative, computationally more efficient, treatment of the target structure exhibit generally good agreement with the experimental data, however, not as good as the correlated two-electron WP-CCC calculations. This must be due to the electron-electron correlation effects accurately included in the two-electron approach. These correlations are included only approximately in the effective one-electron approach. We also find that the difference between the E1E and two-electron WP-CCC results are largest in the elastic-scattering channel. This reflects the fact that the elastic-scattering cross section requires accurate polarizability of the target. The target polarizability is best reproduced in the two-electron WP-CCC approach based on the correlated two-electron target wave function. Other channels are slightly less sensitive to the polarizability. It is concluded that both the correlated two-electron and less expensive effective single-electron WP-CCC approaches are capable of providing a complete and reasonably accurate differential picture of the binary processes taking place in proton-helium collisions. We will next turn our attention to proton-helium differential ionization where there is an abundance of experimental data with which to compare.

[1] D. Tseliakhovich, C. M. Hirata, and K. Heng, Excitation and charge transfer in H-H$^+$ collisions at 5–80 keV and application to astrophysical shocks, Mon. Not. R. Astron. Soc. **422**, 2356 (2012).

[2] O. Marchuk, The status of atomic models for beam emission spectroscopy in fusion plasmas, Phys. Scr. **89**, 114010 (2014).

[3] Dž. Belkić, Review of theories on ionization in fast ion-atom collisions with prospects for applications to hadron therapy, J. Math. Chem. **47**, 1366 (2010).

[4] B. H. Bransden and M. R. C. McDowell, *Charge Exchange and the Theory of Ion-Atom Collisions* (Clarendon Press, Oxford, 1992).

[5] Dž. Belkić, I. Bray, and A. Kadyrov, *State-of-the-Art Reviews on Energetic Ion-Atom and Ion-Molecule Collisions* (World Scientific, Singapore, 2019).

[6] W.-q. Cheng, M. E. Rudd, and Y.-Y. Hsu, Differential cross sections for ejection of electrons from rare gases by 7.5–150-keV protons, Phys. Rev. A **39**, 2359 (1989).

[7] M. R. Flannery and K. J. McCann, Elastic and the 21s and 21p inelastic differential cross sections for proton-helium scattering, J. Phys. B **7**, 1558 (1974).

[8] D. L. Guo, X. Ma, S. F. Zhang, X. L. Zhu, W. T. Feng, R. T. Zhang, B. Li, H. P. Liu, S. C. Yan, P. J. Zhang, and Q. Wang, Angular- and state-selective differential cross sections for single-electron capture in *p*-He collisions at intermediate energies, Phys. Rev. A **86**, 052707 (2012).

[9] T. J. Kvale, D. G. Seely, D. M. Blankenship, E. Redd, T. J. Gay, M. Kimura, E. Rille, J. L. Peacher, and J. T. Park, Angular differential cross sections for the excitation of 1^1S helium to the 2^1S and 2^1P states by 25- to 100-keV-proton impact, Phys. Rev. A **32**, 1369 (1985).

[10] P. J. Martin, D. M. Blankenship, T. J. Kvale, E. Redd, J. L. Peacher, and J. T. Park, Electron capture at very small scattering angles from atomic hydrogen by 25-125-keV protons, Phys. Rev. A **23**, 3357 (1981).

[11] V. Mergel, R. Dörner, K. Khayyat, M. Achler, T. Weber, O. Jagutzki, H. J. Lüdde, C. L. Cocke, and H. Schmidt-Böcking, Strong Correlations in the He Ground State Momentum Wave Function Observed in the Fully Differential Momentum Distributions for the *p* + He Transfer Ionization Process, Phys. Rev. Lett. **86**, 2257 (2001).

[12] J. T. Park and F. D. Schowengerdt, Heavy-particle energy-loss spectrometry: Inelastic cross sections for protons incident upon helium, Phys. Rev. **185**, 152 (1969).

[13] J. T. Park, J. E. Aldag, J. L. Peacher, and J. M. George, Angular Differential Cross Sections for Excitation of Atomic Hydrogen by 25-, 50-, and 100-kev Protons, Phys. Rev. Lett. **40**, 1646 (1978).

[14] J. L. Peacher, T. J. Kvale, E. Redd, P. J. Martin, D. M. Blankenship, E. Rille, V. C. Sutcliffe, and J. T. Park, Elastic differential cross sections for small-angle scattering of 25-, 50-, and 100-keV protons by helium atoms, Phys. Rev. A **26**, 2476 (1982).

[15] M. E. Rudd and T. Jorgensen, Energy and angular distribution of electrons ejected from hydrogen and helium gas by protons, Phys. Rev. **131**, 666 (1963).

[16] M. E. Rudd and D. H. Madison, Comparison of experimental and theoretical electron ejection cross sections in helium by proton impact from 5 to 100 keV, Phys. Rev. A **14**, 128 (1976).

[17] M. Rudd, L. Toburen, and N. Stolterfoht, Differential cross sections for ejection of electrons from helium by protons, At. Data Nucl. Data Tables **18**, 413 (1976).

[18] M. E. Rudd, C. A. Sautter, and C. L. Bailey, Energy and angular distributions of electrons ejected from hydrogen and helium by 100- to 300-keV protons, Phys. Rev. **151**, 20 (1966).

[19] M. S. Schöffler, J. Titze, L. P. H. Schmidt, T. Jahnke, N. Neumann, O. Jagutzki, H. Schmidt-Böcking, R. Dörner, and I. Mančev, State-selective differential cross sections for single and double electron capture in He$^{+,2+}$-He and *p*-He collisions, Phys. Rev. A **79**, 064701 (2009).

[20] M. Schulz, W. T. Htwe, A. D. Gaus, J. L. Peacher, and T. Vajnai, Differential double-excitation cross sections in 50–150-keV proton-helium collisions, Phys. Rev. A **51**, 2140 (1995).

[21] M. Schulz, T. Vajnai, A. D. Gaus, W. Htwe, D. H. Madison, and R. E. Olson, Absolute doubly differential single-ionization cross sections in *p* + He collisions, Phys. Rev. A **54**, 2951 (1996).

[22] M. Schulz, T. Vajnai, and J. A. Brand, Differential double capture cross sections in *p* + He collisions, Phys. Rev. A **75**, 022717 (2007).

[23] D. G. Seely, S. W. Bross, A. D. Gaus, J. W. Edwards, D. R. Schultz, T. J. Gay, J. T. Park, and J. L. Peacher, Angular-differential cross sections for H(2*p*) formation in intermediate-energy proton-helium collisions, Phys. Rev. A **45**, R1287 (1992).

[24] P. N. Abufager, P. D. Fainstein, A. E. Martínez, and R. D. Rivarola, Single electron capture differential cross section in H$^+$+ He collisions at intermediate and high collision energies, J. Phys. B **38**, 11 (2004).

[25] E. Ghanbari-Adivi, Coulomb–born distorted wave approximation applied to the proton–helium single-electron capture process, J. Phys. B **44**, 165204 (2011).

[26] S. Halder, A. Mondal, S. Samaddar, C. R. Mandal, and M. Purkait, Differential and total cross sections for charge transfer and transfer-excitation in ion-helium collisions, Phys. Rev. A **96**, 032717 (2017).

[27] K.-y. Kobayashi and T. Ishihara, Elastic proton-helium scattering in the Glauber approximation, Phys. Rev. A **29**, 3417 (1984).

[28] T. G. Winter, Electron transfer and ionization in proton-helium collisions studied using a Sturmian basis, Phys. Rev. A **44**, 4353 (1991).

[29] A. Henne, H. J. Lüdde, and R. M. Dreizler, Optical potential description of the proton/antiproton-helium collision system, Z. Phys. D **21**, 307 (1991).

[30] C. J. Lundy, R. E. Olson, D. R. Schultz, and J. P. Pascale, Coherence parameters for electron capture in H$^+$ + He collisions, J. Phys. B **27**, 935 (1994).

[31] I. Mancev, V. Mergel, and L. Schmidt, Electron capture from helium atoms by fast protons, J. Phys. B **36**, 2733 (2003).

[32] I. Mančev, N. Milojević, and D. c. v. Belkić, Boundary-corrected four-body continuum-intermediate-state method: Single-electron capture from heliumlike atomic systems by fast nuclei, Phys. Rev. A **91**, 062705 (2015).

[33] R. Potvliege, F. Furtado, and C. Joachain, Multichannel optical mole theory of proton-hydrogen and proton-helium elastic scattering at intermediate energies, J. Phys. B **20**, 1771 (1987).

[34] V. D. Rodríguez, C. A. Ramírez, R. D. Rivarola, and J. E. Miraglia, Helium excitation by protons and highly-charged-ion impact, Phys. Rev. A **55**, 4201 (1997).

[35] D. R. Schultz, C. O. Reinhold, R. E. Olson, and D. G. Seely, Differential cross sections for state-selective electron capture in 25–100-keV proton-helium collisions, Phys. Rev. A **46**, 275 (1992).

[36] H. A. Slim, E. L. Heck, B. H. Bransden, and D. R. Flower, Ionization and charge transfer in proton-helium collisions, J. Phys. B **24**, L421 (1991).

[37] T. G. Wong, M. Foster, J. Colgan, and D. H. Madison, Treatment of ion–atom collisions using a partial-wave expansion of the projectile wavefunction, Eur. J. Phys. **30**, 447 (2009).

[38] X. Guan and K. Bartschat, Complete Breakup of the Helium Atom by Proton and Antiproton Impact, Phys. Rev. Lett. **103**, 213201 (2009).

[39] M. Zapukhlyak, T. Kirchner, A. Hasan, B. Tooke, and M. Schulz, Projectile angular-differential cross sections for transfer and transfer excitation in proton collisions with helium, Phys. Rev. A **77**, 012720 (2008).

[40] M. Baxter and T. Kirchner, Time-dependent density-functional-theory studies of collisions involving he atoms: Extension of an adiabatic correlation-integral model, Phys. Rev. A **93**, 012502 (2016).

[41] S. U. Alladustov, I. B. Abdurakhmanov, A. S. Kadyrov, I. Bray, and K. Bartschat, Wave-packet continuum-discretization approach to proton collisions with helium, Phys. Rev. A **99**, 052706 (2019).

[42] I. B. Abdurakhmanov, A. S. Kadyrov, S. K. Avazbaev, and I. Bray, Solution of the proton-hydrogen scattering problem using a quantum-mechanical two-center convergent close-coupling method, J. Phys. B **49**, 115203 (2016).

[43] I. B. Abdurakhmanov, A. S. Kadyrov, and I. Bray, Accurate solution of the proton-hydrogen three-body scattering problem, J. Phys. B **49**, 03LT01 (2016).

[44] S. K. Avazbaev, A. S. Kadyrov, I. B. Abdurakhmanov, D. V. Fursa, and I. Bray, Polarization of Lyman-α emission in proton-hydrogen collisions studied using a semiclassical two-center convergent close-coupling approach, Phys. Rev. A **93**, 022710 (2016).

[45] I. B. Abdurakhmanov, A. S. Kadyrov, and I. Bray, Wave-packet continuum-discretization approach to ion-atom collisions: Nonrearrangement scattering, Phys. Rev. A **94**, 022703 (2016).

[46] I. B. Abdurakhmanov, J. J. Bailey, A. S. Kadyrov, and I. Bray, Wave-packet continuum-discretization approach to ion-atom collisions including rearrangement: Application to differential ionization in proton-hydrogen scattering, Phys. Rev. A **97**, 032707 (2018).

[47] C. T. Plowman, K. H. Bain, I. B. Abdurakhmanov, A. S. Kadyrov, and I. Bray, Singly differential cross sections for direct scattering, electron capture, and ionization in proton-hydrogen collisions, Phys. Rev. A **102**, 052810 (2020).

[48] I. B. Abdurakhmanov, A. S. Kadyrov, I. Bray, and K. Bartschat, Wave-packet continuum-discretization approach to single ionization of helium by antiprotons and energetic protons, Phys. Rev. A **96**, 022702 (2017).

[49] I. B. Abdurakhmanov, C. T. Plowman, K. H. Spicer, A. S. Kadyrov, and I. Bray, Effective single-electron treatment of ion collisions with multielectron targets without using the independent-event model (unpublished).

[50] I. Abdurakhmanov, O. Erkilic, A. Kadyrov, I. Bray, S. Avazbaev, and A. Mukhamedzhanov, Balmer emission induced by proton impact on atomic hydrogen, J. Phys. B **52**, 105701 (2019).

[51] I. B. Abdurakhmanov, S. U. Alladustov, J. J. Bailey, A. S. Kadyrov, and I. Bray, Proton scattering from excited states of atomic hydrogen, Plasma Phys. Control. Fusion **60**, 095009 (2018).

[52] I. B. Abdurakhmanov, K. Massen-Hane, S. U. Alladustov, J. J. Bailey, A. S. Kadyrov, and I. Bray, Ionization and electron capture in collisions of bare carbon ions with hydrogen, Phys. Rev. A **98**, 062710 (2018).

[53] J. Faulkner, I. Abdurakhmanov, S. U. Alladustov, A. Kadyrov, and I. Bray, Electron capture, excitation and ionization in He^{2+}–H and H$^+$–He$^+$ collisions, Plasma Phys. Control. Fusion **61**, 095005 (2019).

[54] D. Fischer, M. Gudmundsson, Z. Berényi, N. Haag, H. A. B. Johansson, D. Misra, P. Reinhed, A. Källberg, A. Simonsson, K. Støchkel, H. Cederquist, and H. T. Schmidt, Importance of Thomas single-electron transfer in fast p-He collisions, Phys. Rev. A **81**, 012714 (2010).

[55] Hong-Keun Kim, M. S. Schöffler, S. Houamer, O. Chuluunbaatar, J. N. Titze, L. Ph. H. Schmidt, T. Jahnke, H. Schmidt-Böcking, A. Galstyan, Yu. V. Popov, and R. Dörner, Electron transfer in fast proton-helium collisions, Phys. Rev. A **85**, 022707 (2012).